Research Article

Enhancement of Oral Bioavailability and Anti-hyperuricemic Activity of Isoliquiritigenin *via* Self-Microemulsifying Drug Delivery System

Kangyi Zhang,[1] **Qilong Wang,**[1] **Qiuxuan Yang,**[1] **Qiuyu Wei,**[1] **Na Man,**[1] **Michael Adu-Frimpong,**[1] **Elmurat Toreniyazov,**[2,3] **Hao Ji,**[2,4] **Jiangnan Yu,**[1,2,5,6] **and Ximing Xu**[1,2,5,6]

Abstract. The aim of this study was to develop a self-microemulsifying drug delivery system (SMEDDS) for enhancement of the oral bioavailability of isoliquiritigenin (ISL) as well as evaluate its *in vivo* anti-hyperuricemic effect in rats. The ISL-loaded self-microemulsifying drug delivery system (ISL-SMEDDS) was comprised of ethyl oleate (EO, oil phase), Tween 80 (surfactant), and PEG 400 (co-surfactant). The ISL-SMEDDS exhibited an acceptable narrow size distribution (44.78 ± 0.35 nm), negative zeta potential (-10.67 ± 0.86 mV), and high encapsulation efficiency ($98.17 \pm 0.24\%$). The *in vitro* release study indicated that the release rates of the formulation were obviously higher in different release media (HCl, pH 1.2; PBS, pH 6.8; double-distilled water, pH 7.0) compared with the ISL solution. The oral bioavailability of the ISL-SMEDDS was enhanced by 4.71 times in comparison with the free ISL solution. More importantly, ISL-SMEDDS significantly reduced uric acid level by inhibiting xanthine oxidase (XOD) activity in the model rats. Collectively, the prepared ISL-SMEDDS proved to be potential carriers for enhancing the solubility and oral bioavailability of ISL, as well as ameliorating its anti-hyperuricemic effect.

KEY WORDS: Isoliquiritigenin; ISL-SMEDDS; bioavailability; *in vitro* release; anti-hyperuricemic.

INTRODUCTION

Isoliquiritigenin (2, 4, 4′′-trihydroxychalcone, ISL; Fig. 1) is a flavonoid compound with chalcone structure moiety and is mainly found in the root of licorice (*Glycyrrhiza uralensis*) (1), shallots (*Allium ascalonicum*) (2), *Sinofranchetia chinensis* (3), *Dalbergia odorifera* (4), and soybeans (*Glycine max* L.) (5). It has been widely used as active ingredient in pharmaceutical, food, and cosmetic industry (6). Prior

research has demonstrated that ISL possesses diverse pharmacological effects including antioxidant, anti-inflammatory (7), and cytoprotective effects (8), as well as antiplatelet aggregation (9), radical scavenging activity (10), and so on.

As a chalcone-type flavonoid, ISL is very soluble in alkaline aqueous solution and several organic solvents such as ethanol, methanol, chloroform, and ether; however, its solubility in water is low (11). Notably, it has been reported that the low *in vivo* absorption and bioavailability of ISL was due to was due to its poor solubility coupled with the extreme hepatic first-pass effect and rapid elimination (11,12). Consequently, the inherent low solubility and bioavailability of ISL has seriously hindered its clinical applications. Presently, several novel carriers lines have been developed to potentiate the biological activities and improve the bioavailabilities of many nature hydrophobic compounds, which include nanoparticles, liposomes, self-microemulsifying drug delivery system (SEMDDS), and so on (13,14).

SMEDDS possesses immense potential for improving the solubility, absorption, and bioavailability of lipophilic drugs. SMEDDS is thermodynamically stable oily mixture, which is isotropically formed by mixing oils, surfactants, and co-surfactants. It has the ability to form oil-in-water (o/w) microemulsion in a spontaneous manner under mild agitation in gastrointestinal tract (GIT) fluids after oral administration.

Kangyi Zhang and Qilong Wang contributed equally to this work.

Guest Editor: Sanyog Jain

[1] Department of Pharmaceutics, School of Pharmacy, Center for Nano Drug/Gene Delivery and Tissue Engineering, Jiangsu University, Zhenjiang, 212013, People's Republic of China.

[2] Jiangsu Provincial Research Center for Medicinal Function Development of New Food Resources, Zhenjiang, 212001, People's Republic of China.

[3] Tashkent State Agricultural University (Nukus Branch), Avdanberdi Str., Nukus, 742009, Uzbekistan.

[4] Jiangsu Tian Sheng Pharmaceutical Co., Ltd, Zhenjiang, People's Republic of China.

[5] Key Laboratory of Drug Delivery & Tissue Regeneration, Zhenjiang, 212001, People's Republic of China.

[6] To whom correspondence should be addressed. (e–mail: yjn@ujs.edu.cnxmxu@ujs.edu.cn)
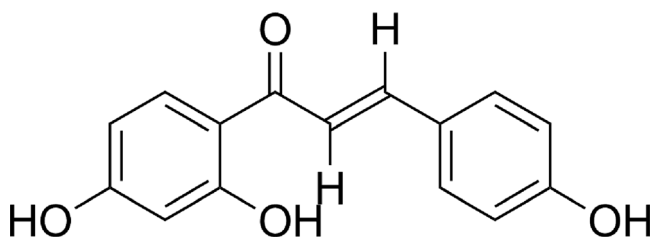
Fig. 1. Chemical structure of ISL

The oil phases of SMEDDS are mostly plant oil and fatty acid ester. The fatty acid ester has good fluidity, dissolution, and self-emulsifying properties with ethyl oleate (EO) being the commonly used as fatty ester in SMEDDS fabrication (15,16). Likewise, the most usually employed non-ionic surfactants (*e.g.*, Tween 80) have relatively high hydrophilic-lipophilic balance (HLB). In order to reduce interfacial tension sufficiently, high concentration of surfactant is needed owing to its ability to cause irritations in GIT. Actually, co-surfactant such as polyethylene glycol 400 (PEG 400) is used to reduce the concentration of surfactant with the capacity to dissolve several hydrophobic drugs and is suitable for oral delivery (17).

Some nanotechnology-based delivery system of ISL like nanostructured lipid carrier (11,18) and liposome (18) have recently been developed to improve the bioavailability and pharmacological activities of the drugs. Nonetheless, SMEDDS offer potential merits over these nanotechnology-based drug delivery systems *via* its ability to improve the absorption of aquaphobic active ingredients by reducing the inherent restriction of incomplete dissolution and facilitating microemulsion formation within the intestines (19). Besides, SMEDDS is thermodynamically stable with ease of fabrication, low cost, and self-emulsifying efficiency (20). It also has the ability to improve the solubility and dissolution rate of scarcely aqueous-soluble drugs by bypassing the first-pass effect and inhibiting P-gp efflux, which result in enhanced intestinal permeability (21,22). Additionally, liquid self-microemulsion preconcentrate enhances lymphatic transportation, provide greater interfacial area for absorption and improve the physical as well as chemical stability of drugs (23). Based on the aforementioned advantages of SMEDDS, the present report sought to develop an effective delivery system for oral administration of ISL with the aim of enhancing the solubility and *in vivo* availability of the drug.

Gout is a metabolic disease caused by long-term disturbance of purine metabolism and elevated serum uric acid (24). An increased uric acid level in the blood is known as hyperuricemia, which is an important biochemical basis of gout characterized by elevated uric acid levels. Xanthine oxidase (XOD) which plays a principal role in gout is an enzyme that converts hypoxanthine to xanthine and subsequently to uric acid. Currently, drugs for gout treatment are mainly divided into drugs inhibiting uric acid production inhibitors (*e.g.*, allopurinol), non-steroidal anti-inflammatory drugs (*e.g.*, indomethacin), and corticosteroids. However, long-term administration of these drugs can cause serious adverse reactions, such as liver and kidney toxicity as well as severe allergic reactions. Therefore, it is essential to unearth natural, safer, and effective drug for the long-term treatment of hyperuricemia and concomitant gouty arthritis. As per our knowledge, the anti-hyperuricemic effect of ISL has not been reported yet.

Herein, ISL-loaded SMEDDS (ISL-SMEDDS) was prepared to improve the solubility and oral *in vivo* availability of the drug. An optimum preparation ratio of ISL-SMEDDS was consequently developed and characterized through appropriate indices (droplet size, morphology by transmission electron microscopy-TEM, entrapment efficiency-EE, drug loading-DL, and the stability). The *in vitro* drug release and pharmacokinetic investigations of the ISL-SMEDDS were subsequently conducted. Besides, rat model of hyperuricemia was established *via* intraperitoneal injection of potassium oxalate and intragastric administration of hypoxanthine and was employed to evaluate the anti-hyperuricemic activity of ISL-SMEDDS.

MATERIALS AND METHODS

Materials

ISL (purity 98%) was obtained from Langze Pharmaceutical Technology Co., Ltd. (Nanjing, China). Hydrochloric acid (HCl) and phosphate-buffered saline (PBS) were bought from Sinopharm Chem, Reagent Co., Ltd. (Shanghai, China). EO was supplied by Guangfu Fine Chem Research Inst. (Tianjin, China). Tween 80 and PEG 400 were obtained from Sinopharm Chemical Reagent Co., Ltd. (Shanghai, China). Acetanilide (ACE), potassium oxazine, uric acid standard, allopurinol, and xanthine oxidase assay kit were bought from Aladdin Industrial Corp., (Shanghai, China). Methanol (chromatographically pure) was provided by Honeywell Burdick & Jackson (Muskegon, MI, USA). Double-distilled water (DDW) was made in-house with a Millipore water purifying system (Millipore Corporation, Bedford, MA, USA). Other chemicals reagents were obtained commercially and were of analytical grade.

The Laboratory Animal Centre of Jiangsu University (Zhenjiang, China) supplied the male Sprague-Dawley (SD) rats (200 ± 20 g).

Preparation of ISL-SMEDDS

The ISL-SMDEDDS was prepared through a previously reported method (25,26), while pre-formulation was conducted to select the appropriate excipients. Briefly, ISL (86.40 mg) was mixed with EO (155.44 mg), tween 80 (660.09 mg) and PEG 400 (178.07 mg). Magnetic stirrer was applied to stir the mixture at 37°C for 60 s to obtain stable and uniform ISL-SMEDDS. After dilution with DDW (100 mL) and stirring, the obtained formulation solution was stored at room temperature until further analyses.

In Vitro HPLC Method for Determination of ISL

In vitro HPLC method for analyzing ISL-SMEDDS was established in-house. The HPLC system consisted of an UV detector, 1260 Quat Pump, 1260 ALS, 1260 TCC (1260 LC, Agilent, USA) and 1260 DAD VL as well as a C18 column (5 μm, 4.6 × 150 mm, Agilent, USA). The analytical conditions were as follows, mobile phase was methanol-water mixture (60/40, *v/v*) as mobile phase, column temperature was at 30°C, detection wavelength was set at 372 nm, flow rate of 1.0 mL/min and the injection volume was 20 μL. The analysis

method was validated to be suitable for detecting of ISL with the standard curve demonstrating a good linearity. The regression equation was $A = 143.86C + 9.3748$ ($R^2 = 0.999$, $n = 8$, linear range from 0.05 to 100 μg/mL).

ISL-SMEDDS Characterization

Physical Characterization

ISL-SMEDDS (1 mg/ml) was diluted with DDW prior to the physical indices measurement. The droplet size (DS), polydispersity index (PDI), and zeta potential (ZP) were determined with dynamic and phase analysis light scattering (DLS and PALS, respectively) technique using NanoBrook 90Plus PALS (Brookhaven Instruments Corporation, Holtsville, NY, USA). The measurements were recorded in triplicates at 25°C and 90° angle of scattering angle.

Morphology Characterization

Morphology of ISL-SMEDDS (1 mg/mL) was observed through transmission electron microscopy (TEM). An aliquot of diluted ISL-SMEDDS (20 μL, 500 μg/mL) was placed on a copper-grid and dyed with 2% phosphotungstic acid. After air-drying, the obtained thin-film was observed using TEM (JEM-2100, JEOL, Tokyo, Japan).

EE and DL of ISL-SMEDDS

The EE and DL of the formulated ISL was determined as described in earlier work (27). The prepared ISL-SMEDDS (1 mg/mL, 1 mL) was placed in centrifugal filters (30KDa, Amicon Ultra-15, Millipore, Germany) and centrifuged at 7378×g for 20 min (5804, Eppendorf, Germany) to separate the unincorporated ISL. Absolute methanol was used to dilute the filtrate to yield a final solution (10 mL). Aliquot of the solution (20 μL) was injected into RP-HPLC for determination of the amount of ISL. The EE and DL were estimated *via* the following equation:

$$\text{EE\%} = \frac{C_{\text{total}} - C_{\text{free-ISL}}}{C_{\text{total}}} \times 100\%$$
$$\text{DL\%} = \frac{(C_{\text{total}} - C_{\text{free-ISL}}) \times V}{W_{\text{lipids}}} \times 100\%$$

The $C_{\text{free ISL}}$ represents the quantity of unincorporated ISL in self-microemulsion (after filtration), whereas C_{total} denotes total amount of ISL in SMEDDS. Also, V represents the volume of formulated ISL-SMEDDS in one recipe, and W_{lipid} represents the weight of the vehicle.

Stability of ISL-SMEDDS

The stability study of the formulated ISL-SMEDDS was performed at various storage times, and the variations in the DS, PDI, and ZP were assessed. Samples were kept in airtight tubes (glass) and were stored for 3 months at accelerated condition (temperature at 40 ± 2°C, relatively humidity 75 ± 5%). At the respective months (0, 1, 2, and 3), the mean DS, PDI, and ZP were evaluated to establish assess the storage stability of ISL-SMEDDS.

In addition, the samples were stored in sealed tubes at room temperature for 1 month. Within a month (0, 15, 30 days), samples were extracted at predetermined intervals. The mean DS, PDI, and zeta potential were evaluated in triplicate.

In Vitro Drug Release Study

Prior to the release study, the solubility of ISL in various media was investigated. Excess amount of ISL was dissolved in 3 mL of each media (pH 1.2 HCl, pH 6.8 PBS, pH 7.0 DDW and pH 7.4 PBS). Thermostatic oscillator operating at constant temperature (37 ± 0.5°C) and speed (100 rpm) was used to conduct the solubility test. After 72 h, each sample was centrifuged for 10 min at 7378×g, diluted for ten-fold and the concentration of ISL was analyzed after injecting into HPLC.

The *in vitro* drug release profiles of ISL in differential media were measured by dialysis diffusion method with slight modifications (Pharmacopeia of China, 2015), while three parallel experiments were conducted. Briefly, ISL solution (0.5 mg/mL, 1 mL) and ISL-SMEDDS (equivalent ISL amount) were respectively placed in dialysis bags (MV 3500D, 25 mm × 5 m, Shanghai Green Bird Science and Technology Development, China), under the condition of leaky groove, tied at each end, and then placed in various release media (pH 1.2 HCl, pH 7.0 DDW, and pH 6.8 PBS). Water-bath vibrator with constant conditions (37 ± 0.5°C and 100 rpm) was used to conduct the release test with total release media volume of 400 mL. Periodically, samples (1 mL each) were taken from the various media at 0.08, 0.25, 0.5, 1, 2, 4, 6, 8, 10, 12, and 24 h and accordingly replaced with the same volume and type of fresh media to maintain the *sink* condition. HPLC method (described in the "*In Vitro* HPLC Method for Determination of ISL" section) was used to analyze the samples.

Bioavailability Study

In Vivo HPLC Conditions

The HPLC system comprised of a 1260 Quat Pump, 1260 ALS, 1260 TCC, and 1260 DAD VL (Agilent, USA). The analytical conditions were as follows: Symmetry C18 column (5 μm, 4.6 × 150 mm, Agilent, USA) set at 30°C, methanol-water mixture (60/40, *v/v*) as mobile phase with a flow rate of 1.0 mL/min. A 254-nm absorption wavelength was used to detect internal standard (acetanilide) and 372 nm absorption wavelength was used for ISL detection. Likewise, ISL was detected at a wavelength of 254 nm during the first 0–3 min but was detected at 372 nm from 3 to 10 min. This method was selected on the account of previous report (28). Standard plasma solution comprising of ISL (blank plasma spiked with ISL standards) was prepared using desired concentrations (0.1, 0.2, 1, 2, 5, and 10 μg/mL). The ISL content was plotted on horizontal axis (x) and that of peak areas on the vertical axis (y). The standard curve of ISL *in vivo*: $y = 0.9378x - 0.16$ ($n = 6$, $R^2 = 0.998$), with concentration linearly ranged (0.1–10 μg/mL).

Treatment of Plasma Sample

Liquid-liquid extraction method was employed to extract ISL from rats' plasma as stated in a previous report (29). In brief, plasma (200 μL) was mixed with 20 μL of Acetanilide (50 μg/mL, internal standard), then 600 μL of ethyl acetate was added to extract the drug from plasma. The ethyl acetate layer was cautiously removed and combined after repeated extraction (twice). After drying under nitrogen gas with mild heat, the residue was dissolved in methyl alcohol (400 μL) and centrifuged for 10 min at 7378×g. The supernatant was analyzed with HPLC system.

In Vivo Pharmacokinetics Study of ISL-SMEDDS

The male Sprague-Dawley (SD) rats (200 ± 20 g) used in this study were supplied by the Laboratory Animal Centre of Jiangsu University (Zhenjiang, China). The protocol for the experiment was in compliance with Jiangsu University's Ethics Committee and guidelines spelt out for animal study by National Institute for Care and Use of Laboratory Animals (UJS-IACUC-2019032202). Prior to the experiment, the rats (12) were randomly separated into two groups, namely free ISL group and ISL-SMEDDS group with six rats in each group. The animals were kept in standard rodent house and were fasted for 12 h before experiment (given free access to water). Each rat in the two groups was orally administered with the same dose (200 mg/kg) of free ISL (suspended in 0.5% sodium carboxy-methyl-cellulose solution) and ISL-SMEDDS, respectively. Blood samples (0.5 mL each) were collected from the eye-orbit area with capillaries at different times (0.1, 0.25, 0.5, 1, 2, 3, 4, 6, 8, 10, 12, and 24 h) after administration. Plasma was obtained from whole blood after centrifuging for 10 min at 1010×g and was stored at − 20°C prior to further analysis. Treatment of plasma samples was described in section 2.6.2. The main pharmacokinetic parameters, *viz.* the maximum peak concentrations (C_{max}), time to reach this concentration (T_{max}), mean residence time (MRT), and the area under the concentration-time curve ($AUC_{0-\infty}$) were computed with the BAPP 2.3 pharmacokinetic software (supplied by the Center of Drug Metabolism of China Pharmaceutical University, Nanjing, China). The equation for computing relative oral bioavailability (F_r) of the drug was as follows:

$$F_r = \frac{AUC_T}{AUC_R} \times 100\%$$

where AUC_T and AUC_R denote the area under the concentration-time curve of the ISL-loaded SMEDDS and ISL solution, respectively.

Anti-hyperuricemic Activities of ISL in Rats

Establishment of Rat Model of Hyperuricemia

The male SD rats (200 ± 20 g) model of hyperuricemia was established (30) by intraperitoneal injection of potassium oxalate emulsion (25 mg/mL, 10 mL/kg) and intragastric administration of hypoxanthine suspension (100 mg/mL, 10 mL/kg).

Serum Uric Acid HPLC Conditions

The level of serum uric acid in rats was determined using a Shimadzu HPLC UV detector (LC-20 CE, Shimadzu, Japan) and equipped with a Symmetry®C18 column (4.6 mm × 250 mm, 5 μm; Waters, USA) at 30°C. The mobile phase was 0.2% acetic acid aqueous solution/methanol (94/6, *v/v*) with a flow rate of 1.0 mL/min, and an aliquot (20 μL) of the sample was injected into HPLC and was detected at 288 nm wavelength for detection. The plasma (100 μL) was spiked with different concentrations of uric acid (1, 2.5, 5, 10, 15, and 20 μg/mL). Regression analysis was carried out with uric acid concentration as abscissa and peak area as ordinate.

Determination of Serum Uric Acid and Xanthine Oxidase Activity

Fifty-four male SD rats were randomly divided into nine groups (*n* = 6), namely normal control group (NC), model control group (MC), positive control group (PC, 40 mg/kg, allopurinol), ISL low-dose group (I-L, 50 mg/kg), ISL medium-dose group (I-M, 100 mg/kg), ISL high-dose group (I-H, 150 mg/kg), ISL-SMEDDS low-dose group (I-S-L, 50 mg/kg), ISL-SMEDDS medium-dose group (I-S-M, 100 mg/kg), and ISL-SMEDDS high-dose group (I-S-H, 150 mg/kg). One hour (1 h) after the establishment of hyperuricemic model, each animal in the NC and MC groups was intragastrically administered with 3 mL of physiological saline (0.9%), while PC groups were treated with allopurinol (25 mg/kg), and each rat in the other six groups was intragastrically administered with 3 mL of various doses of free ISL and ISL-SMEDDS. After 3 h, blood samples (1 mL each) were collected from the eye-orbit area with capillaries and determination of serum uric acid by HPLC.

Presumably, XOD catalyzes the oxidation of xanthine to uric acid. Therefore, inhibition of XOD activity is an effective strategy for the treatment of hyperuricemia. Determination of XOD activity in serum and liver was achieved using commercial test kit by Nanjing Jiangcheng Bioengineering Institute.

Histopathological Examination

All the rats were executed, and their liver and kidney were collected and fixed with 4% paraformaldehyde at 4°C for 24 h. After washing with PBS (pH 7.4), the samples were embedded in paraffin, sliced at 5 μm, and stained with hematoxylin and eosin. The prepared samples were observed under a microscope (Nikon, Japan).

Statistical Analysis

The entire experimental data were presented as mean ± SD (standard deviation). The differences among groups were statistically analyzed ascertained with Student's t test *via* the SPSS software (version 13.0 SPSS Company, USA). The statistically significance level was considered at $p < 0.05$.
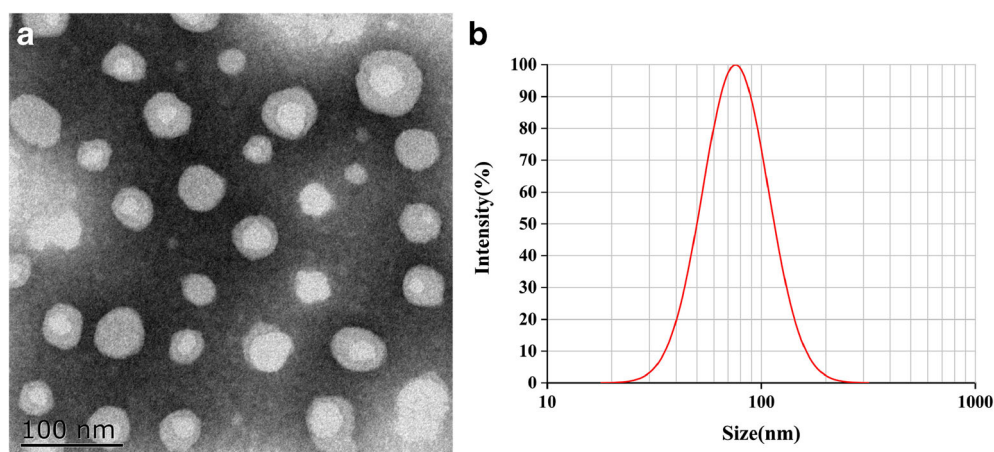
Fig. 2. a, b The TEM image and droplet size distribution of ISL-SMEDDS

RESULT AND DISCUSSION

Characterization of ISL-SMEDDS

The mean DS of the prepared ISL-SMEDDS diameter was 44.78 ± 0.35 nm (Fig. 2b) with PDI of 0.20 ± 0.01 while the ZP was − -10.67 ± 0.86 mV. As shown in Fig. 2a, the ISL-SMEDDS was nearly spherically in shaped with smooth surface and homogenous size while without any sign of droplet agglomeration. The EE% of the formulation was 98.17 ± 0.24, which was in line with previous report (31). The DL of the SMEDDS formulation was 7.69 ± 0.02%.

Usually, DS is an important index for evaluating the quality of nanoformulations as size of particles could impact on the rate and extent of drug release, thereby affecting the intestinal absorptions and bioavailability of active ingredients (32). This is because as the diameter of particle reduces, the interfacial surface for drug absorption also increases (33). Previous investigations have proved that smaller DS could contribute to enhanced drug absorption and oral bioavailability of drugs after administration (34,35). The DS of ISL-SMEDDS prepared in the present study was less than 50 nm, which accord with the classification of microemulsion. The small particle size of ISL-SMEDDS might also contribute to the improvement of ISL absorption *in vivo* (36). The lower PDI also portrayed further the homogeneousness of the globule size in the nanodispersion (37). As a parametric measure of stability, a higher ZP is considered ideal for a stable formulation. A ZP of − 10.67 mV obtained for ISL-SMEDDS agree with previous report (38,39). Pertinently, SMEDDS formulations with ZP above − 10 mV has been observed to be stable (38). Collectively, these findings

Table I. The Results of Accelerated Stability of ISL-SMEDDS (Mean ± SD, $n = 3$)

Time (months)	Particle size (nm)	Zeta potential (mV)	PDI
0	44.78 ± 0.35	− 10.00 ± 0.29	0.20 ± 0.01
1	45.90 ± 0.86	− 9.76 ± 0.69	0.21 ± 0.01
2	47.88 ± 0.91	− 8.12 ± 0.17	0.21 ± 0.01
3	50.31 ± 0.47	− 7.90 ± 0.52	0.23 ± 0.02

PDI polydispersity index

suggest the stability of ISL-SMEDDS, which is prerequisite for the delivery of the drug. The EE and DL results demonstrated that high amount of ISL was successfully incorporated in the SMEDDS and may have the potential to improve the ISL absorption *in vivo*.

Stability Studies

Various reports (40,41) have described that 3 months of stability study can be used to preliminarily prove the stability of the preparation. Table I showed the storage stability result of ISL-SMEDDS for 3 months at accelerated condition. There was no statistical significance in the variation of DS, ZP, and PDI, suggesting that the ISL-SMEDDS was acceptably stable under the prevailing condition for the storage period. These results showed that the formulation of ISL-SMEDDS was uniform and stable for *in vivo* applications. It can be observed from Table I that there was an increase in DS and ZP over time. The increase in DS could be due to the aggregation of the droplets with time. Usually ZP is the potential between the droplet surface and the dispersed liquid, which varies with the distance between the ion and the droplet surface (42). A decrease of zeta potential value indicates probable coalescence of the ISL-SMEDDS droplets. This is consistent with the phenomenon of change in particle size. Moreover, the change in DS and ZP during the 3 months study was statistically insignificant ($p > 0.5$).

Additionally, the stability of ISL-SMEDDS at room temperature was also studied for 1 month to assess effect of temperature on the stability of the formulation and the results is shown in Table II. It can be inferred from the Table II that the DS, ZP, and PDI of ISL-SMEDDs did not change significantly during storage at room temperature (30 days). The results showed that the preparation could be preserved stably under the above conditions.

In Vitro Release of ISL-SMEDDS

As shown in Fig. 3, the solubility of ISL in pH 1.2, pH 6.8, pH 7.0, and pH 7.4 were 4.58 ± 0.46 µg/mL, 3.85 ± 0.31 µg/mL, 6.09 ± 0.55 µg/mL, and 7.64 ± 0.57 µg/mL, respectively. The results revealed that ISL demonstrated different solubility pattern at the various pH condition with high solubility in PBS (pH 7.4).

Table II. The Results of Stability of ISL-SMEDDS at Room Temperature (Mean ± SD, $n = 3$)

Time (day)	Particle size (nm)	Zeta potential (mV)	PDI
0	44.43 ± 0.45	− 10.54 ± 0.31	0.19 ± 0.01
15	45.11 ± 0.19	− 10.20 ± 0.45	0.19 ± 0.02
30	45.04 ± 0.14	− 10.25 ± 0.31	0.20 ± 0.01

PDI polydispersity index

The *in vitro* release results showed that the drug was released faster from SMEDDS than free drug solution. As depicted in Fig. 4, the cumulative release rates of ISL from ISL-SMEDDS in the three media were significantly higher than that of the free ISL solution in the three media. It was also observed that the cumulative release ratio of ISL from SMEDDS within 24 h in pH 1.2 HCl, pH 6.8 PBS, and pH 7.0 DDW reached 78.95%, 66.41%, and 82.34% respectively. Meanwhile, only 51.08%, 46.87%, and 58.68% of total ISL were released from free ISL in the three media, respectively. Relatively higher release rate of ISL from SMEDDS compared with the free drug (nearly 80% in DDW and in PBS) indicated that the solubility of ISL was improved. The smaller DS of the ISL-SMEDDS might have contributed to the improvement in the ISL solubility in both DDW and PBS (31). Therefore, smaller globule size usually results in increased the surface area, which in turn might have enhanced the release of ISL. These finding indicated that the formulation could facilitate the movement of ISL through the GI mucous membrane (43). The surfactant and co-surfactants incorporated in the microemulsion system could undermine the membrane permeability, thereby improving the wettability and water solubility of the compound (44). Thus, the ISL-loaded SMEDDS system has the prospect of improving the bioavailability of ISL *in vivo*. Actually, at nearly neutral pH (similar to intracellular and/or intestinal environments), SMEDDS formulations considerably influence the biopharmaceutical properties of the lipophilic drugs *via* increased dissolution rate and solubility (45). The high solubility of ISL-SMEDDS in water could probably be
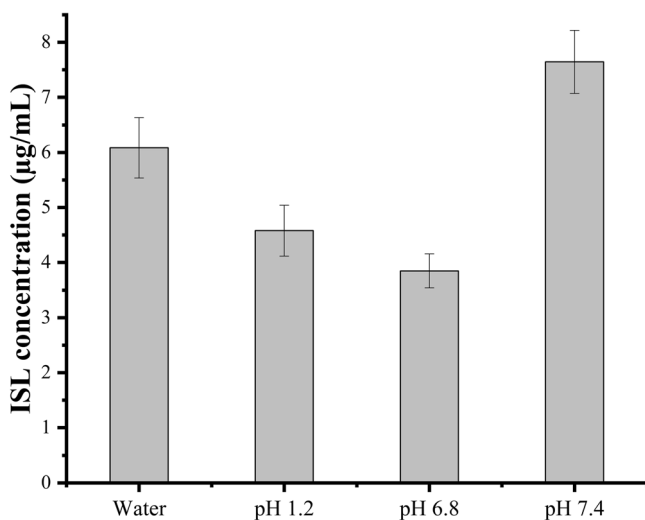
ascribed to the ability of the system to form fine oil-in-water microemulsions upon contact with aqueous phase *via* gentle agitation by the thermostatic oscillator (46). On the other hand, the difference of release curves between pH 6.8 PBS and pH 1.2 HCl might be due to the successful encapsulation of ISL in self-microemulsion and thus are protected from the effect of gastric acid environment. There was no sudden release in these three media, which indicated that the prepared preparation is uniform, and the drug was successfully loaded into the drug.

Pharmacokinetic Analysis of ISL-SMEDDS

The plasma drug concentration-time profiles of pure ISL and ISL-SMEDDS after oral administration of a single dose (200 mg/kg) are presented in Fig. 5, and the pharmacokinetic parameters were calculated and are displayed in Table III. The figure depicted that plasma drug concentration of ISL-SMEDDS was obviously higher than the free ISL. Likewise, the observed profile displayed that plasma drug concentration of ISL-SMEDDS was remarkably higher than the free ISL.

The pharmacokinetic variables were evaluated with the BAPP 2.3 pharmacokinetic software with the result was displayed in Table III. The C_{max} (0.46 ± 0.02 μg/mL) and $AUC_{0-24\ h}$ (2.72 ± 0.26 μg/mL) of free ISL was significantly lower compared with the ISL-SMEDDS (1.24 ± 0.14 μg/mL and 12.81 ± 1.40 μg/mL, respectively). These results indicated that *in vivo* absorption of ISL was markedly enhanced by SMEDDS (p < 0.01), which correlated with the *in vitro* release results. The bioavailability of ISL-SMEDDS was significantly higher than the unformulated ISL after single oral dosing with the relative bioavailability increasing by 4.71 times.

The values of area-under-the concentration-time curve ($AUC_{0-24\ h}$) coupled with the C_{max} values showed that *in vivo* ISL-SMEDDS absorption was substantially higher ($p < 0.01$) than that of the unformulated drug. Moreover, the MRT of ISL-SMEDDS (9.73 ± 0.06 h) were longer than the unformulated ISL (7.04 ± 0.09 h), which means that the prepared SMEDDS could increase the systemic circulation of ISL in the body. The possible reason for enhanced bioavailability observed in the formulated drug profile could be ascribable to direct nanodroplet uptake *via* the GIT and increased permeability by surfactants (47), as well as decreased degradation and clearance. Therefore, the carrier improved the solubility and bioavailability of the ISL, thereby justifying its appropriateness for oral administration. The ISL-loaded SMEDDS exhibited double peak phenomenon, which is characterized by an initial increase profile to reach a first peak that begun to decline and then raised again to attain a second peak which was higher than the first. The observed pattern of plasma concentration *versus* time profiles in rats was not dose-dependent. There were two peaks for both free ISL and ISL-SMEDDS, which showed that the characteristic pattern may be due to the occurrence of enterohepatic circulation (48). Previous report indicated that ISL is mainly absorbed in the GI membrane *via* passive diffusion. The double peak phenomenon of ISL could be attributed to the absorption variability within different regions of the gut and is thought to be the most probable physiological explanation for this pattern (18). Further investigations are therefore needed to clarify the double peak phenomenon of ISL in details.

Fig. 3. The solubility of ISL in various media
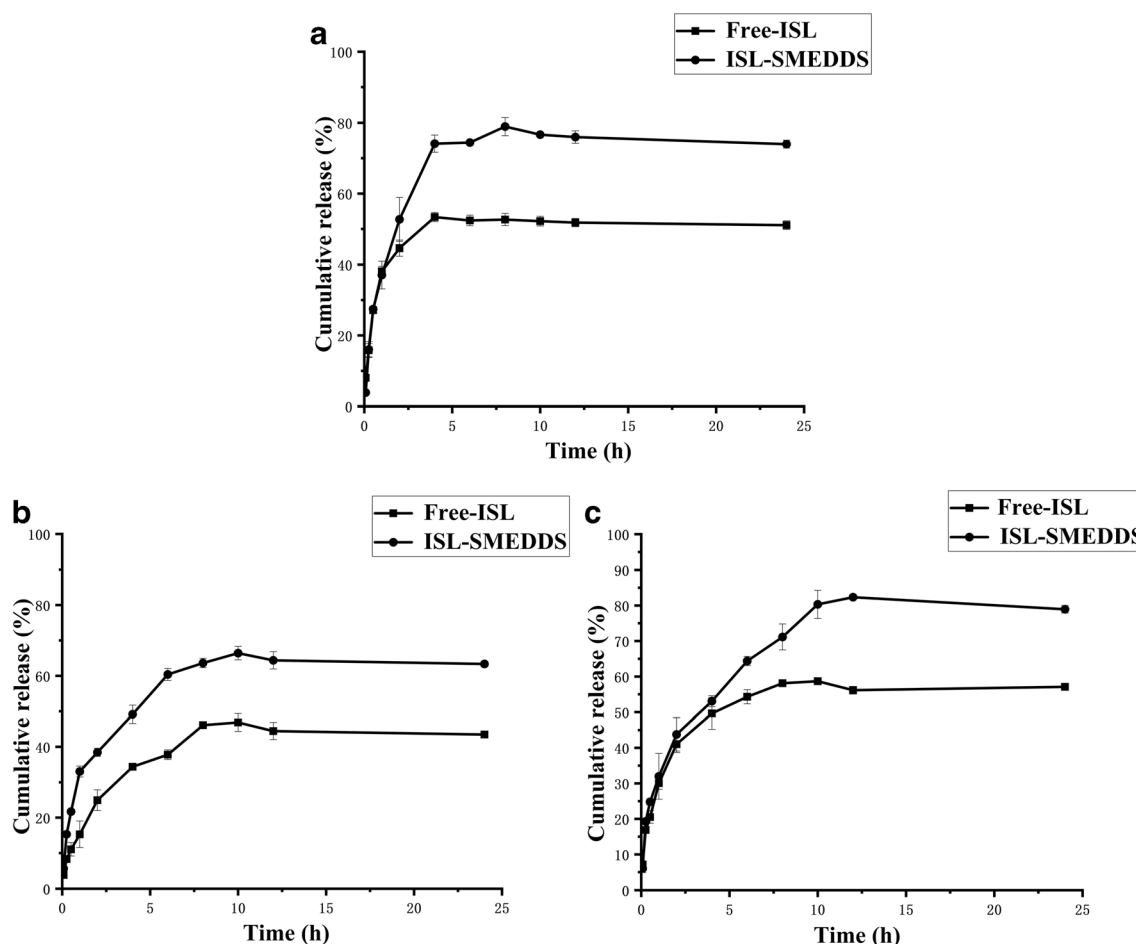
Fig. 4. In vitro release profiles of ISL from free ISL and ISL-SMEDDS in different medium compared: **a** in vitro release profile of free ISL aLnd and ISL-SMEDDS in HCl solution (pH 1.2); **b** in vitro release profile of free ISL and ISL-SMEDDS in PBS (pH 6.8); **c** in vitro release profile of free ISL and ISL-SMEDDS in double-distilled water (pH 7.0) (mean ± SD, n = 3)

Effect of ISL-SMEDDS on Uric Acid in Rats

As shown in Fig. 6, the uric acid value of the model group was significantly higher than that of other groups, which indicated that
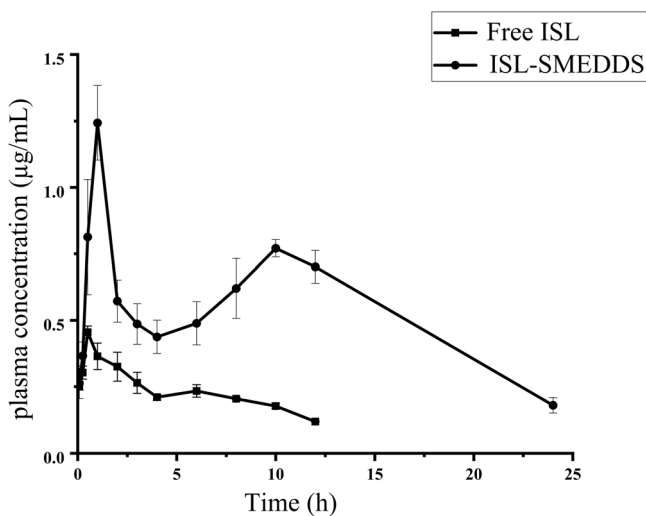

Fig. 5. Plasma concentration profile of free ISL and ISL-SMEDDS (mean ± SD, n = 6)

the model of hyperuricemia rats was successfully established. Compared with the MC group, the level of serum uric acid was decreased in both the ISL-SMEDDS and the free ISL. Notably, three different doses (50, 100,150 mg/kg) of ISL-SMEDDS significantly reduced serum uric acid levels by 41.76%, 61.20%, and 78.83%, respectively compared with the MC group. With the increase dosage of ISL-SMEDDS, uric acid value decreased

Table III. Pharmacokinetic Parameters of Free ISL and ISL-SMEDDS After Oral Administration (Mean ± SD, $n = 6$) in Rats

Parameters	Free ISL	ISL-SMEDDS
$AUC_{0-36\,h}$ (μg/mL)	2.72 ± 0.26	12.81 ± 1.40**
C_{max} (μg/mL)	0.46 ± 0.02	1.24 ± 0.14**
$T_{1/2}$ (h)	8.14 ± 0.46	24.07 ± 0.83**
MRT_{0-t} (h)	7.04 ± 0.09	9.73 ± 0.06**
T_{max} (h)	0.5 ± 0	1 ± 0

ISL isoliquiritigenin, *ISL-SMEDDS* ISL-loaded self-microemulsifying drug delivery system, *AUC* area under the concentration-time curve, *C_max* maximum peak concentrations, *T_1/2* half-life, *MRT* mean residence time, *T_max* time to reach maximum concentration

*p < 0.05, compared with free ISL; **p < 0.01, compared with free ISL
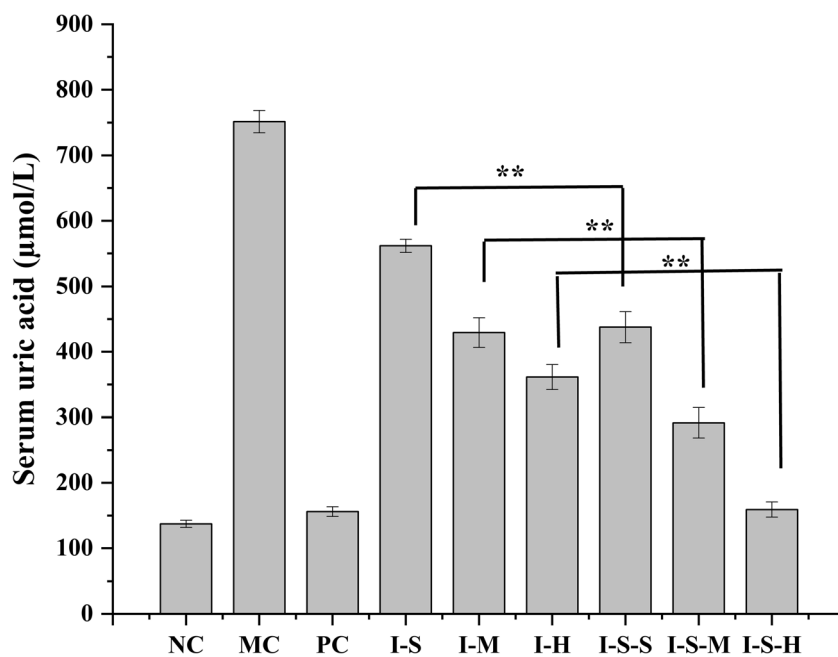
Fig. 6. The levels of the serum uric acid. **$p < 0.05$, ISL-SMEDDS compared with free -ISL

significantly, which was dose-dependent. More importantly, the same doses of free ISL also decreased serum uric acid level ($p < 0.05$) by about 25.27%, 42.88%, and 51.92%, respectively. The serum uric acid value of ISL-SMEDDS was close to that of PC, which indicted that ISL-SMEDDS had similar uric acid-lowering activity as allopurinol. These results suggest that the ISL-SMEDDS can significantly improve the anti-hyperuricemia activity of ISL.

## ISL Reduces Uric Acid by Inhibiting XOD Activity

The possible mechanism of ISL in reducing uric acid was explored by detecting the activity of XOD in serum and liver of rats. XOD activity in serum and liver of rats with hyperuricemia was inhibited by allopurinol and the three doses of ISL as shown in Fig. 7. The results indicated that
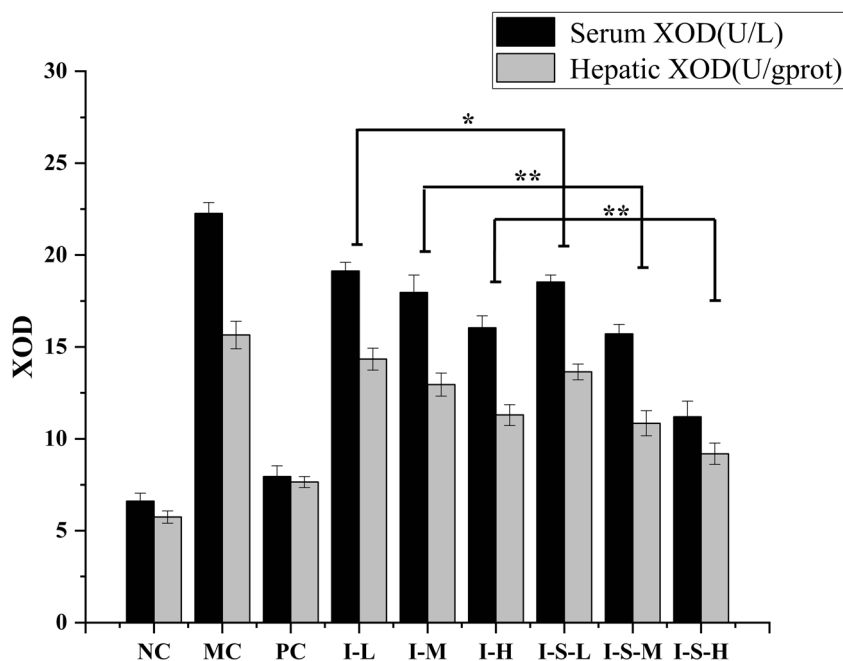

Fig. 7. The XOD activity in serum and hepatic in various groups. Normal control group (NC); model control group (MC); positive control group (PC); ISL low-dose group (I-L, 50 mg/kg); ISL medium-dose group (I-M, 100 mg/kg); ISL high-dose group (I-H, 150 mg/kg); ISL-SMEDDS low-dose group (I-S-L, 50 mg/kg); ISL-SMEDDS medium-dose group (I-S-M, 100 mg/kg); ISL-SMEDDS high-dose group (I-S-H, 150 mg/kg). *$p < 0.1$, **$p < 0.05$. compared with free ISL

Liver
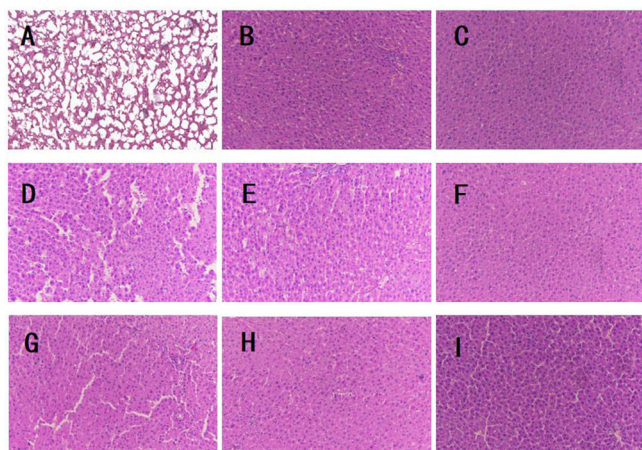
Kidney
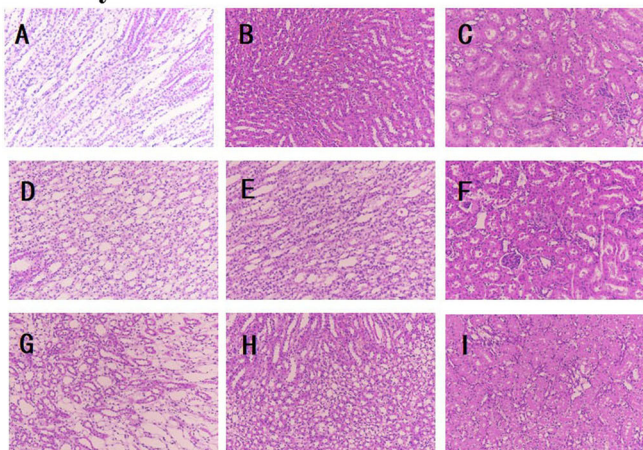
Fig. 8. Histopathological analysis of the liver and kidney in rats treated with different therapies: **A** MC (model control group); **B** NC (normal control group); **C** PC (positive control group); **D** I-L (ISL low-dose group); **E** I-M (ISL medium-dose group); **F** I-H (ISL high-dose group); **G** I-S-L (ISL-SMEDDS low-dose group); **H** I-S-M (ISL-SMEDDS medium-dose group); **I** I-S-H (ISL-SMEDDS high-dose group)

each of the doses of ISL inhibited XOD activity compared with the model group. The XOD activity in liver and serum of ISL-SMEDDS (the low-dose group) was lower than that of the free ISL ($p < 0.1$). Likewise, XOD activities in liver and serum of ISL-SMEDDS (the middle-dose group and high-dose group) were significantly lower than that of the free ISL ($p < 0.05$). In hyperuricemic rats, a dosage (150 mg/kg) of ISL-SMEDDS inhibited XOD activity in serum and liver by 35.50% and 41.27% respectively. Likewise, free ISL (14.03% and 8.40% accordingly) also inhibited XOD activity; however, the degree of inhibition was lower than that of the ISL-SMEDDS. In the I-S-H group, the inhibition of XOD activity was close to the positive drug. This indicated that ISL-SMEDDS could reduce XOD activity close to normalcy.

Histopathological Analysis

Studies have shown that hyperuricemia is associated with liver and kidney damage (49). As indicated in Fig. 8, there were obvious pathological changes such as edema, necrosis and degeneration in the MC compared with the NC, suggesting that hyperuricemia may damage the liver and kidney of rats. However, organs of the rats treated with free ISL and ISL-SMEDDS showed different degrees of histomorphological recovery. More importantly, the tissue morphology of I-S-H group was close to NC, which suggests that ISL-SMEDDS has better organ repair effect than free ISL. These results suggested that ISL-SMEDDS could effectively improve the organ protection of ISL in hyperuricemic rats.

CONCLUSIONS

In this study, ISL-loaded SMEDDS was successfully prepared to improve the water solubility and oral bioavailability of ISL, a poorly aqueous-soluble compound with various pharmacological effects. Characterization of ISL-SMEDDS showed that it has smaller and narrowed droplet size, negative zeta potential, and high drug entrapment efficiency. The *in vitro* release results suggested that the solubility of ISL was remarkably improved by SMEDDS. After oral administration of free

ISL and ISL-SMEDDS in rats, the results demonstrated that the SMEDDS markedly enhanced the plasma concentration as well as oral bioavailability of ISL. Moreover, ISL-SMEDDS could significantly reduce serum uric acid value level by inhibiting XOD activity. Collectively, these results provide preliminary information on possible clinical application of ISL and other similar water-insoluble compounds.

COMPLIANCE WITH ETHICAL STANDARDS

The protocol for the experiment was in compliance with Jiangsu University's Ethics Committee and guidelines spelt out for animal study by National Institute for Care and Use of Laboratory Animals (UJS-IACUC-2019032202).

Conflict of Interest The authors declare that they have no conflict of interest.

REFERENCES

1. Cuendet M, Guo J, Luo Y, Chen S, Oteham CP, Moon RC, et al. Cancer chemopreventive activity and metabolism of isoliquiritigenin, a compound found in licorice. Cancer Prev Res. 2010;3:221–32.
2. Yaling H, Chunchieh C, Chen PJ, Huang SE, Huang SC, Polin K. Shallot and licorice constituent isoliquiritigenin arrests cell cycle progression and induces apoptosis through the induction

of ATM/p53 and initiation of the mitochondrial system in human cervical carcinoma HeLa cells. Mol Nutr Food Res. 2010;53:826–35.

3. Pan X, Kong LD, Zhang Y, Cheng CHK, Tan RX. In vitro inhibition of rat monoamine oxidase by liquiritigenin and isoliquiritigenin isolated from Sinofranchetia chinensis. Acta Pharmacol Sin. 2000;21:949–53.

4. Lee SH, Kim JY, Seo GS, Kim YC, Sohn DH. Isoliquiritigenin, from Dalbergia odorifera , up-regulates anti-inflammatory heme oxygenase-1 expression in RAW264.7 macrophages. Inflamm Res. 2009;58:257–62.

5. Cao JH, Wang Y, Ji C, Ye JN. Determination of liquiritigenin and isoliquiritigenin in Glycyrrhiza uralensis and its medicinal preparations by capillary electrophoresis with electrochemical detection. J Chromatogr A. 2004;1042:203–9.

6. Kundu P, Neese S, Bandara S, et al. The effects of the botanical estrogen, isoliquiritigenin on delayed spatial alternation. Neurotoxicol Teratol. 2018;66:55–62.

7. Li, B.; Liu, B.; Li, J.; Xiao, H.; Wang, J.; Liang, G. Experimental and theoretical investigations on the supermolecular structure of isoliquiritigenin and 6-O-α-d-maltosyl-β-cyclodextrin inclusion complex. Int J Mol Sci. 2015;16:17999–18017.

8. Zhang, D. H.; Lan-Lan, Y. E.; Cheng, H.; Wei, Y. U.; Yang, J. Cytoprotective effect and its mechanisms of isoliquiritigenin on acetaminophen induced acute injury of hepatocytes. CJCPT. 2008;13:293-298.

9. Radnaabazar C, Park CM, Kim JH, Cha J, Song YS. Fibrinolytic and antiplatelet aggregation properties of a recombinant Cheonggukjang kinase. J Med Food. 2011;14:625–9.

10. Poullain C, Girard-Valenciennes E, Smadja J. Plants from Reunion Island: evaluation of their free radical scavenging and antioxidant activities. J Ethnopharmacol. 2004;95:19–26.

11. Zhang XY, Qiao H, Ni JM, Shi YB, Qiang Y. Preparation of isoliquiritigenin-loaded nanostructured lipid carrier and the in vivo evaluation in tumor-bearing mice. Eur J Pharm Sci. 2013;49:411–22.

12. Qiao H, Zhang X, Wang T, Liang L, Chang W, Xia H. Pharmacokinetics, biodistribution and bioavailability of isoliquiritigenin after intravenous and oral administration. Pharm Biol. 2014;52:228–36.

13. Zhang, X.; Hua, Q.; Zhang, T.; Shi, Y.; Ni, J. Enhancement of gastrointestinal absorption of isoliquiritigenin by nanostructured lipid carrier. Adv Power Technol. 2014;25:1060–8.

14. Zhou, J. X.; Lin, W. U.; Wang, J. G. Technology preparation of isoliquiritigenin microcapsule and their release in vitro. Mod Food Sci Tech. 2010;10:1132-5.

15. Lu, J. L.; Wanga, J. C.; Liu, X. Y., et al. Self-microemulsifying drug delivery system (SMEDDS) improves anticancer effect of oral 9-nitrocamptothecin on human cancer xenografts in nude mice. Eur J Pharm Biopharm. 2008;69:899–907.

16. Chen, C.; Cai, D.; Qin, P.; Chen, B.; Wang, Z.; Tan, T. Bioplasticizer production by hybrid acetone-butanol-ethanol fermentation with full cell catalysis of Candida sp. 99–125. Bioresour Technol. 2018; 257:217-22.

17. Al BGE. SMEDDS: a novel approach for lipophilic drugs. Int J Pharm Sci. 2012;3:2441-2450.

18. Zhang X, Qiao H, Zhang T, Shi Y, Ni J. Enhancement of gastrointestinal absorption of isoliquiritigenin by nanostructured lipid carrier. Adv Powder Technol. 2014;25:1060–8.

19. W N, C. Lipids, lipophilic drugs, and oral drug delivery-some emerging concepts. J Pharm Sci. 2000;89:967–978.

20. Shakeel, F.; Alanazi, F. K.; Raish, M.; Haq, N.; Radwan, A. A.; Alsarra, I. A. Pharmacokinetic and in vitro cytotoxic evaluation of cholesterol-rich nanoemulsion of cholesteryl-succinyl-5-fluorouracil. Jour Mol Liq. 2015; 211:164–168.

21. Mezghrani, O.; Ke, X.; Bourkaib, N.; Xu, B. H. Optimized self-microemulsifying drug delivery systems (SMEDDS) for enhanced oral bioavailability of astilbin. Pharmazie. 2011;66:754–60.

22. Zhang YR, He L, Yue SL, Huang QT, Zhang YH, Yang JY. Characterization and evaluation of a self-microemulsifying drug delivery system containing tectorigenin, an isoflavone with low aqueous solubility and poor permeability. Drug Delivery. 2017;24:632–40.

23. Bedi N, Sharma K, Singh D. Tacrolimus loaded liquid and solid self-microemulsion preconcentrates: development and evaluation. Drug Delivery Letters. 2017;7:24–38.

24. Ragab, G.; Elshahaly, M.; Bardin, T. Gout: an old disease in new perspective—a review. J Adv Res. 2017;8:495-511.

25. Yi C, Zhong H, Tong S, Cao X, Firempong CK, Liu H, et al. Enhanced oral bioavailability of a sterol-loaded microemulsion formulation of Flammulina velutipes, a potential antitumor drug. Int J Nanomedicine. 2012;7:5067–78.

26. Yao, J.; Lu, Y.; Zhou, J. Preparation of nobiletin in self-microemulsifying systems and its intestinal permeability in rats. J Pharm Pharm Sci. 2008;11:22–29.

27. Zhu J, Wang Q, Li H, Zhang H, Zhu Y, Omari-Siaw E, et al. Galangin-loaded, liver targeting liposomes: optimization and hepatoprotective efficacy. J Drug Deli Sci Tech. 2018;46:339–47.

28. Xie, Y. J.; Wang, Q. L.; Adu-Frimpong, M., et al. Preparation and evaluation of isoliquiritigenin-loaded F127/P123 polymeric micelles. Drug Devel Ind Pharm. 2019;1:29.

29. Zhu Y, Peng W, Zhang J, Wang M, Firempong CK, Feng C, et al. Enhanced oral bioavailability of capsaicin in mixed polymeric micelles: preparation, in vitro and in vivo evaluation. J Funct Foods. 2014;8:358–66.

30. Yang QX, Wang QL, Deng WW, et al. Anti-hyperuricemic and anti-gouty arthritis activities of polysaccharide purified from Lonicera japonica in model rats. Int J Biol Macromol. 2019;123:801–9.

31. Qureshi MJ, Mallikarjun C, Kian WG. Enhancement of solubility and therapeutic potential of poorly soluble lovastatin by SMEDDS formulation adsorbed on directly compressed spray dried magnesium aluminometasilicate liquid loadable tablets: a study in diet induced hyperlipidemic rabbits. Asi J Pharm Sci. 2015;10:40–56.

32. Truong DH, Tran TH, Ramasamy T, Choi JY, Lee HH, Moon C, et al. Development of solid self-emulsifying formulation for improving the oral bioavailability of erlotinib. AAPS PharmSciTech. 2016;17:466–73.

33. 33. Gu Z, Shi X, Omari-Siaw E, Zhu Y, Li H, Guo M, et al. Self-microemulsifying sustained-release pellet of Ginkgo biloba extract: preparation, invitro drug release and pharmacokinetics study in beagle dogs. J Drug Deli Sci Tech. 2017;37:184–93.

34. Dixit AR, Rajput SJ, Patel SG. Preparation and bioavailability assessment of SMEDDS containing valsartan. AAPS PharmSciTech. 2010;11:314–21.

35. Zhu Y, Zhang J, Zheng Q, Wang M, Deng W, Li Q, et al. In vitro and in vivo evaluation of capsaicin-loaded microemulsion for enhanced oral bioavailability. J Sci Food Agri. 2015;95:2678–85.

36. Wang Q, Wei Q, Yang Q, Cao X, Li Q, Shi F, et al. A novel formulation of [6]-gingerol: proliposomes with enhanced oral bioavailability and antitumor effect. Int J Pharm. 2018;535:**308**–15.

37. Shi F, Wei Z, Zhao Y, Xu X. Nanostructured lipid carriers loaded with baicalin: an efficient carrier for enhanced antidiabetic effects. Pharmacogn Mag. 2016;12:198.

38. Balata, G. F.; Essa, E. A.; Shamardl, H. A.; Zaidan, S. H.; Abourehab, M. A. Therapy self-emulsifying drug delivery systems as a tool to improve solubility and bioavailability of resveratrol. Drug Des Devel Ther. 2016; 10:117–28.

39. Bajaj, A.; Rao, M. R.; Khole, I.; Munjapara, G. Self-nanoemulsifying drug delivery system of cefpodoxime proxetil containing tocopherol polyethylene glycol succinate. Drug Dev Ind Pharm. 2013;39:635–45.

40. Bachhav, Y. G.; Patravale, V. B. SMEDDS of glyburide: formulation, in vitro evaluation, and stability studies. AAPS PharmSciTech. 2009;10:482-7.

41. Parmar, N. Study of cosurfactant effect on nanoemulsifying area and development of lercanidipine loaded (SNEDDS) self nanoemulsifying drug delivery system. Colloids Surf B Biointerfaces. 2011;86:327–338.

42. Qureshi, M. J.; Mallikarjun, C.; Kian, W. G. Enhancement of solubility and therapeutic potential of poorly soluble lovastatin by SMEDDS formulation adsorbed on directly compressed spray dried magnesium aluminometasilicate liquid loadable tablets: a study in diet induced hyperlipidemic rabbits. Asia J

Pharm Sci. 2015;10:40–56.

43. Zhu Y, Wang M, Zhang J, Peng W, Firempong CK, Deng W, et al. Improved oral bioavailability of capsaicin via liposomal nanoformulation: preparation, in vitro drug release and pharmacokinetics in rats. Arch Pharm Res. 2015;38:512–21.

44. Xia WJ, Onyuksel H. Mechanistic studies on surfactant-induced membrane permeability enhancement. Pharm Res. 2000;17:612–8.

45. Gupta, S.; Kesarla, R.; Omri, A. Formulation strategies to improve the bioavailability of poorly absorbed drugs with special emphasis on self-emulsifying systems. ISRN Pharm. 2013;2013:848043.

46. Parul, J.; Geeta, A.; Sasidharan Leelakumari, H.; Kashmir, S. Development of self-microemulsifying drug delivery system and solid-self-microemulsifying drug delivery system of telmisartan. Int J Pharm Investig. 2014;4:195–206.

47. Shi F, Zhao Y, Firempong CK, Xu X. Preparation, characterization and pharmacokinetic studies of linalool-loaded nanostructured lipid carriers. Pharm Biol. 2016;54:2320–8.

48. Wang Y, Wang S, Firempong CK, et al. Enhanced solubility and bioavailability of naringenin via liposomal nanoformulation: preparation and in vitro and in vivo evaluations. AAPS PharmSciTech. 2016;18:1–9.

49. Kumar P, Das A, Savant SS, Mandal RK, Hassan S. Gout nodulosis: report of a rare case and brief review. Dermatol Online J. 2015;21:8.